nature biotechnology

Kinetic fingerprinting to identify and count single nucleic acids

Alexander Johnson-Buck[1,8,9], Xin Su[2,9], Maria D Giraldez[3], Meiping Zhao[2], Muneesh Tewari[3–7] & Nils G Walter[1]

MicroRNAs (miRNAs) have emerged as promising diagnostic biomarkers. We introduce a kinetic fingerprinting approach called single-molecule recognition through equilibrium Poisson sampling (SiMREPS) for the amplification-free counting of single unlabeled miRNA molecules, which circumvents thermodynamic limits of specificity and virtually eliminates false positives. We demonstrate high-confidence, single-molecule detection of synthetic and endogenous miRNAs in both buffer and minimally treated biofluids, as well as >500-fold discrimination between single nucleotide polymorphisms.

© 2015 Nature America, Inc. All rights reserved.

Stable, diagnostically useful miRNAs have recently been detected in blood and other body fluids, but reproducible quantification of circulating miRNAs has proven challenging[1]. Standard assays based on amplification by polymerase chain reaction (PCR), although highly sensitive, require time-consuming extraction and amplification steps. Next-generation sequencing approaches enable high-throughput profiling of RNA transcripts, but cannot reliably quantify low-abundance analytes (**Supplementary Note 1**). Although a number of sensitive, amplification-free nucleic acid assays have been reported[2–5], these typically suffer from significant false positives and/or strict limits on target specificity imposed by the thermodynamics of hybridization[6] (**Supplementary Note 1**).

Here we present a technique for the amplification-free, single-molecule detection of unlabeled RNA biomarkers that circumvents many of the above issues. The SiMREPS approach is inspired by the super-resolution imaging technique DNA-PAINT[7] and exploits the direct binding of a short (9- to 10-nucleotide, nt) fluorescently labeled DNA probe to an unlabeled miRNA analyte immobilized on a glass surface (**Fig. 1a**). Using total internal reflection fluorescence (TIRF) microscopy[8,9], both specific binding to the immobilized target and nonspecific surface binding are detected (**Supplementary Fig. 1**). However, the equilibrium binding of the probe to the target yields a distinctive kinetic signature, or fingerprint, that can be used to achieve ultra-high discrimination against background binding (**Fig. 1b**,**c**). Because the kinetics of exchange for probes of ~6–12 nt are highly sensitive to the number of complementary bases between the probe and target[7,10,11], varying the length of the probe allows fine-tuning of the kinetic behavior to improve specificity of detection. For the probes used in this study, kinetics of binding and dissociation were found to be more closely correlated to probe length than to the melting temperature of the duplex (**Supplementary Fig. 2**).

As the transient binding of probes to an immobilized target can be idealized as a Poisson process, the s.d. in the number of binding and dissociation events (N_{b+d}) is expected to increase only as $\sqrt{N_{b+d}}$, implying that the observation time can be lengthened to achieve arbitrarily high discrimination between target and off-target binding (**Supplementary Note 2**). Consistent with this expectation, as the experimental acquisition time is increased, the signal and background peaks in histograms of N_{b+d} are progressively better resolved (**Fig. 1d**), and the width of the signal distribution increases only as $\sqrt{N_{b+d}}$ (**Supplementary Fig. 3**). Note that the choice of probe length is critical to achieve this separation on convenient experimental time scales (**Supplementary Fig. 4**).

To test the generality of SiMREPS, we evaluated four human miRNAs that are dysregulated in cancer and other diseases[12–14], *hsa-let-7a*, *hsa-miR-21*, *hsa-miR-16* and *hsa-miR-141*, and one non-human miRNA from *Caenorhabditis elegans*, *cel-miR-39* (**Supplementary Fig. 5**). Although the binding kinetics varied among the target-probe pairs, the signal and background peaks were well-separated for all targets (**Supplementary Fig. 5b**); by stipulating a threshold of $N_{b+d} \geq 15$, empirically perfect discrimination (specificity = 1) was achieved (**Supplementary Fig. 5e**). Standard curves constructed using this threshold for the five miRNAs show a linear dependence on target concentration of over two to three orders of magnitude (**Fig. 1e**).

Because the lifetime of a short DNA duplex increases as an approximately exponential function of the number of base pairs[7,10,11], we reasoned that SiMREPS might be used to achieve excellent single-base discrimination. To test this hypothesis, we used a single fluorescent probe to discriminate between two *let-7* family members, *hsa-let-7a* and *hsa-let-7c*. We found that the lifetime of the probe-bound state τ_{on} differed by a factor of ~4.7 for the two targets, whereas the unbound-state lifetime τ_{off} showed no target dependence (**Fig. 2a**,**b**). Photobleaching is much slower than probe dissociation under our illumination conditions (**Supplementary Fig. 6**). With the standard acquisition time of 10 min, *let-7a* and *let-7c* could be distinguished

[1]Single Molecule Analysis Group, Department of Chemistry, University of Michigan, Ann Arbor, Michigan, USA. [2]Beijing National Laboratory for Molecular Sciences, MOE Key Laboratory of Bioorganic Chemistry and Molecular Engineering, College of Chemistry and Molecular Engineering, Peking University, Beijing, China. [3]Department of Internal Medicine, Division of Hematology/Oncology, University of Michigan, Ann Arbor, Michigan, USA. [4]Department of Internal Medicine, Division of Molecular Medicine and Genetics, University of Michigan, Ann Arbor, Michigan, USA. [5]Department of Biomedical Engineering, University of Michigan, Ann Arbor, Michigan, USA. [6]Center for Computational Medicine and Bioinformatics, University of Michigan, Ann Arbor, Michigan, USA. [7]Biointerfaces Institute, University of Michigan, Ann Arbor, Michigan, USA. [8]Present address: Department of Cancer Biology, Dana-Farber Cancer Institute, Boston, Massachusetts, USA. [9]These authors contributed equally to this work. Correspondence should be addressed to N.G.W. (nwalter@umich.edu).

Received 22 March; accepted 7 May; published online 22 June 2015; doi:10.1038/nbt.3246

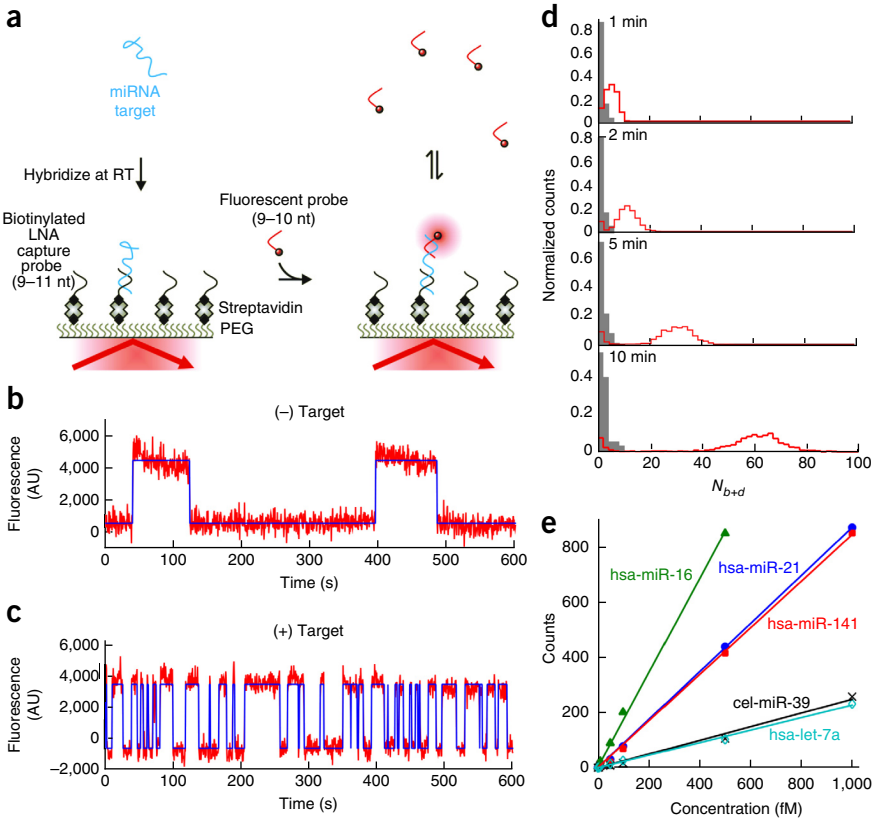

Figure 1 High-confidence detection of miRNAs with SiMREPS. (**a**) Experimental approach of SiMREPS detection of miRNAs. An immobilized miRNA target is identified by fluorescence microscopy as the site of repeated transient binding by short fluorescent DNA probes. (**b**,**c**) Binding of probes to the slide surface (**b**) exhibits kinetic behavior distinct from that of binding to a target molecule (**c**) (red, fluorescence intensity; blue, idealization from hidden Markov modeling). (**d**) Histograms of the number of candidate molecules showing a given number of intensity transitions (N_{b+d}) in the absence (gray) or presence (red) of 1 pM *miR-141* with varying acquisition times. (**e**) Standard curves from SiMREPS assays of five miRNAs. Linear fits were constrained to a *y*-intercept of 0, yielding R^2 values < 0.99.

at the single-copy level with a discrimination factor >100 at >96% sensitivity, or with a discrimination factor >570 (beyond the limit of quantification in this experiment) at ~70% sensitivity (**Fig. 2b**,**c** and **Supplementary Fig. 7**). Not only is this substantially larger than the typical discrimination factors of 2–100 reported for single mismatches using other hybridization-based probes[2,4,6,15], but as SiMREPS achieves discrimination at the single-molecule level, it is possible to independently quantify a target and a point mutant with high confidence in a mixture containing both species.

The high sensitivity and specificity of SiMREPS suggest that it may be capable of high-confidence RNA detection in complex biological matrices. To test this notion, we used SiMREPS to detect *hsa-let-7a* in a HeLa whole-cell extract. The N_{b+d} histogram for endogenous *hsa-let-7a* showed a well-defined peak (**Fig. 2d**), similar to that observed for synthetic *hsa-let-7a* (**Supplementary Fig. 5a**) and *hsa-let-7c* (**Supplementary Fig. 7**), which vanished in the presence of an LNA (locked nucleic acid) *let-7* inhibitor designed to bind and sequester *let-7* family members. Notably, dwell time analysis of the fluorescent

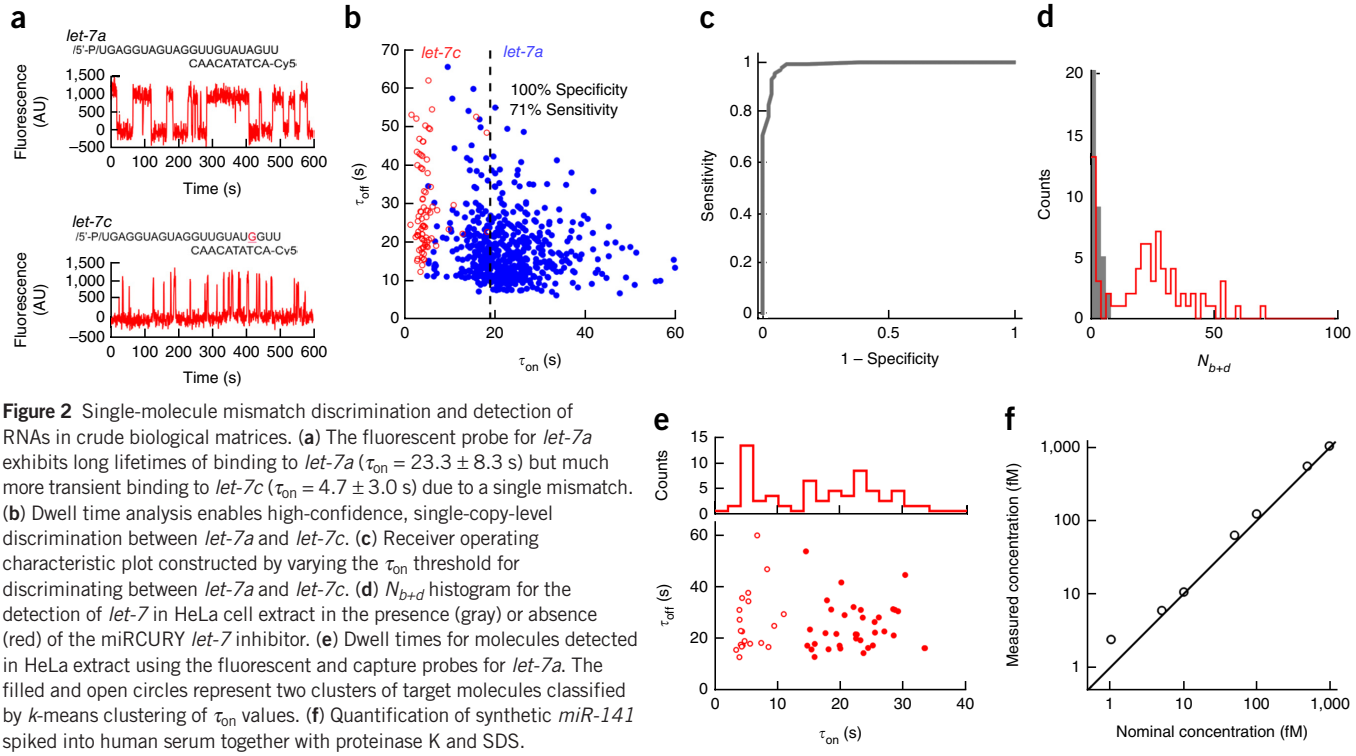

Figure 2 Single-molecule mismatch discrimination and detection of RNAs in crude biological matrices. (**a**) The fluorescent probe for *let-7a* exhibits long lifetimes of binding to *let-7a* (τ_{on} = 23.3 ± 8.3 s) but much more transient binding to *let-7c* (τ_{on} = 4.7 ± 3.0 s) due to a single mismatch. (**b**) Dwell time analysis enables high-confidence, single-copy-level discrimination between *let-7a* and *let-7c*. (**c**) Receiver operating characteristic plot constructed by varying the τ_{on} threshold for discriminating between *let-7a* and *let-7c*. (**d**) N_{b+d} histogram for the detection of *let-7* in HeLa cell extract in the presence (gray) or absence (red) of the miRCURY *let-7* inhibitor. (**e**) Dwell times for molecules detected in HeLa extract using the fluorescent and capture probes for *let-7a*. The filled and open circles represent two clusters of target molecules classified by *k*-means clustering of τ_{on} values. (**f**) Quantification of synthetic *miR-141* spiked into human serum together with proteinase K and SDS.

© 2015 Nature America, Inc. All rights reserved.

probe binding events yielded two populations of molecules that were readily resolved by *k*-means clustering of the τ_{on} values (**Fig. 2e**) and are consistent with the expected τ_{on} distributions for *hsa-let-7a* and *hsa-let-7c*.

To investigate whether SiMREPS can detect miRNAs of clinical interest in minimally treated biofluids, we conducted the assay for the prostate cancer biomarker *hsa-miR-141* (ref. 16) in a serum sample from a healthy individual after spiking in varying concentrations of synthetic *hsa-miR-141* together with SDS and proteinase K to protect against RNase activity (**Supplementary Fig. 8**). The measured concentration (calibrated from **Fig. 1e**) was strongly correlated with the nominal spiked-in concentration (**Fig. 2f**, $R > 0.999$, slope = 1.07). Consistent with the expected low concentration (0.1–5 fM) of *miR-141* in the serum of healthy individuals[16], we measured a concentration of 0.4 ± 0.5 fM (s.e.m., $n = 3$) in this serum specimen in the absence of spiked-in synthetic *miR-141*.

We have presented a method for the rapid, high-confidence, direct detection and quantification of specific nucleic acid biomarkers with transiently binding probes. SiMREPS lends itself to miniaturization, multiplexing and extension to non-TIRF, microscopy-based detection approaches[17,18], so we expect it to find broad application in both clinical diagnostics and research.

METHODS

Methods and any associated references are available in the online version of the paper.

Note: Any Supplementary Information and Source Data files are available in the online version of the paper.

ACKNOWLEDGMENTS

This work was funded in part by the Department of Defense MURI Award W911NF-12-1-0420 (to N.G.W.) and US National Institutes of Health Transformative R01 grant R01DK085714 (to M.T.). X.S. acknowledges support from the China Scholarship Council. M.D.G. acknowledges initial support from a Rio Hortega Fellowship and later from a Martin Escudero Fellowship.

The authors thank A.M. Chinnaiyan, M. Bitzer, A. Sahu, S. Pitchiaya, L.A. Heinicke and M.L. Kahlscheuer for helpful discussions. The authors acknowledge J.D. Hoff and the Single-Molecule Analysis in Real-Time (SMART) Center for instrumentation and assistance in TIRF microscopy measurements.

AUTHOR CONTRIBUTIONS

N.G.W. and A.J.-B. conceived the idea. A.J.-B., N.G.W. and X.S. designed the experiments. X.S. and A.J.-B. carried out experiments and analyzed the results. A.J.-B., N.G.W., X.S., M.T., M.D.G. and M.Z. interpreted the results and wrote the paper.

COMPETING FINANCIAL INTERESTS

The authors declare competing financial interests: details are available in the online version of the paper.

Reprints and permissions information is available online at http://www.nature.com/reprints/index.html.

1. Schwarzenbach, H., Hoon, D.S.B. & Pantel, K. *Nat. Rev. Cancer* **11**, 426–437 (2011).
2. Gunnarsson, A., Jonsson, P., Marie, R., Tegenfeldt, J.O. & Hook, F. *Nano Lett.* **8**, 183–188 (2008).
3. Geiss, G.K. *et al. Nat. Biotechnol.* **26**, 317–325 (2008).
4. Li, L., Li, X., Li, L., Wang, J. & Jin, W. *Anal. Chim. Acta* **685**, 52–57 (2011).
5. Ho, S.-L., Chan, H.-M., Ha, A.W.-Y., Wong, R.N.-S. & Li, H.-W. *Anal. Chem.* **86**, 9880–9886 (2014).
6. Zhang, D.Y., Chen, S.X. & Yin, P. *Nat. Chem.* **4**, 208–214 (2012).
7. Jungmann, R. *et al. Nano Lett.* **10**, 4756–4761 (2010).
8. Axelrod, D., Burghardt, T.P. & Thompson, N.L. *Annu. Rev. Biophys. Bioeng.* **13**, 247–268 (1984).
9. Walter, N.G., Huang, C.-Y., Manzo, A.J. & Sobhy, M.A. *Nat. Methods* **5**, 475–489 (2008).
10. Cisse, I.I., Kim, H. & Ha, T. *Nat. Struct. Mol. Biol.* **19**, 623–627 (2012).
11. Dupuis, N.F., Holmstrom, E.D. & Nesbitt, D.J. *Biophys. J.* **105**, 756–766 (2013).
12. Lu, M. *et al. PLoS ONE* **3**, e3420 (2008).
13. Ruepp, A. *et al. Genome Biol.* **11**, R6 (2010).
14. Russo, F. *et al. PLoS ONE* **7**, e47786 (2012).
15. Garcia-Schwarz, G. & Santiago, J.G. *Angew. Chem. Int. Ed.* **52**, 11534–11537 (2013).
16. Mitchell, P.S. *et al. Proc. Natl. Acad. Sci. USA* **105**, 10513–10518 (2008).
17. Sorgenfrei, S. *et al. Nat. Nanotechnol.* **6**, 126–132 (2011).
18. Baaske, M.D., Foreman, M.R. & Vollmer, F. *Nat. Nanotechnol.* **9**, 933–939 (2014).

© 2015 Nature America, Inc. All rights reserved.

ONLINE METHODS

Oligonucleotides. All miRNA samples were purchased from Integrated DNA Technologies with a 5′-phosphate modification and high-performance liquid chromatography (HPLC) purification, except for *let-7a* and *let-7c*, which were purchased from Dharmacon with a 5′-phosphate modification, deprotected according to the supplier's instructions, and purified by reversed-phase C_{18} HPLC (Varian ProStar 210, Waters SunFire C18). All DNA probes were purchased from IDT and HPLC-purified by the manufacturer. LNA capture probes were purchased from Exiqon with HPLC purification.

Single-molecule fluorescence microscopy. SiMREPS experiments were performed using either a previously described prism-type TIRF microscope[19] (HeLa extract experiments) or a Olympus IX-81 objective-type TIRF microscope equipped with a 60 × oil-immersion objective (APON 60XOTIRFM, 1.49NA) as well as Cell^TIRF and z-drift control modules (all other experiments). For prism-type TIRF microscopy experiments, fluidic sample cells were constructed using two pieces of double-sided tape sandwiched between a quartz slide and glass coverslip as previously described[19] (**Supplementary Fig. 9a**). For objective-type TIRF microscopy measurements, sample cells were constructed by fixing a cut 1-cm length of a pipet tip (Eppendorf) to a coverslip using epoxy adhesive (Double Bubble, Hardman Adhesives; **Supplementary Fig. 9b**). In either case, imaging surface (quartz slide or coverslip) was coated with a 1:10 mixture of biotin-PEG-5000 and mPEG-5000 (Laysan Bio, Inc.) immediately before construction of the sample cell as previously described[20]. Prepared slides were stored in the dark for up to 2 weeks.

SiMREPS quantification of synthetic miRNAs. Quantification of synthetic miRNA targets by SiMREPS was performed as follows. All miRNA handling was performed in GeneMate low-adhesion 1.7-ml microcentrifuge tubes, and dilutions for standard curves were performed in the presence of 0.03 mg/ml oligo(dT_{10}) (Integrated DNA Technologies) as a carrier. The slide surface was briefly incubated with T50 buffer (10 mM Tris-HCl, 1 mm EDTA, pH 8.0) followed by 1 mg/ml streptavidin. After 10 min, excess streptavidin was flushed out by three volumes of T50. The surface was then incubated with 20 nM of the appropriate biotinylated LNA capture probe (Exiqon, Inc.) in 1× PBS buffer for 10 min, and the excess flushed out by three volumes of 1× PBS. A 100-µl portion of target RNA (*hsa-let-7a*, *hsa-miR-16*, *hsa-miR-21*, *cel-miR-39* or *hsa-miR-141*) was introduced into the sample chamber and incubated for 10 min (prism-type TIRF microscopy) or 60 min (objective-type TIRF microscopy). The longer incubation time for the objective-type TIRF microscopy measurements was necessary because of the tall (~1 cm) sample cell, which slowed the transport of analyte to the imaging surface. An imaging buffer containing 4× PBS, 2.5 mM 3,4-dihydroxybenzoate, 25 nM protocatechuate dioxygenase, 1 mM Trolox[21], and 25 nM of the Cy3- or Cy5-labeled fluorescent probe was added to the sample chamber. The transient binding of probes to captured target molecules was monitored for 10 min under illumination by 532 nm and/or 640 nm laser light. Image acquisition was performed at a rate of 2 Hz using an iCCD camera (iPentamax:HQ Gen III, Roper Scientific, MCP gain 70) for measurements of *let-7* in HeLa extract, and an EMCCD camera (IXon 897, Andor, EM gain 1000) for all other measurements.

Detection of endogenous *let-7* in crude HeLa extract. A 5-µl aliquot of HeLa whole cell extract (from Thermo Scientific In-Vitro Protein Expression Kit, #88881) was incubated for 5 min at room temperature in the presence of 0 or 1.7% (w/v) sodium dodecyl sulfate (SDS) and 0 or 140 nM miRCURY *let-7* inhibitor (Exiqon). We found that SDS treatment was essential for detection of endogenous *let-7* in HeLa extract; all data shown in **Figure 2d–e** resulted from experiments in the presence of SDS. The lysate was vortexed, diluted 100-fold in 4× PBS imaging buffer containing 25 nM of the fluorescent probe for *hsa-let-7a*, and added to a microscope slide coated with an excess of the LNA capture probe. After a10-min incubation, the transient binding of the fluorescent probe was observed by prism-type TIRF microscopy for 10 min as described above.

Detection of synthetic *miR-141* spiked into crude serum. 50 µl of freshly thawed human serum (BioreclamationIVT, #BRH844152) was combined with SDS (final 2% w/v), proteinase K (New England BioLabs, Inc., P8107S; final concentration 0.16 units/µl), and synthetic *hsa-miR-141*, and incubated for 15 min at room temperature. Next, EDTA was added to a final concentration of 20 mM, and the sample heated to 90 °C in a copper bath for 2 min. After cooling to room temperature for 5 min, each sample was allowed to bind to the microscope coverslip surface for 1 h. Residual serum was removed, the surface washed with 1× PBS, and imaging carried out by objective-type TIRF microscopy as described above. The measured concentration of *miR-141* was calculated using the standard curve collected in buffer (**Fig. 1e**).

Analysis of SiMREPS data. Custom MATLAB code was used to identify sites of fluorescent probe binding and calculate intensity-versus-time trajectories from the CCD movie. Intensity trajectories were subjected to hidden Markov modeling (HMM) using QuB[22] in order to identify the number of binding and/or dissociation events (N_{b+d}) and mean dwell times in the bound (τ_{on}) and unbound (τ_{off}) states for each candidate molecule. Based on control measurements in absence of target, a threshold of $N_{b+d} = 15$ (6 s.d. above background) was used to identify target molecules. Additional filtering criteria were used to reject spurious transitions detected by the HMM software: to be counted as a target molecule, a candidate must (i) have a mean bound-state intensity signal at least 2.5 s.d. and 1,000 counts above the mean background intensity, and (ii) exhibit median values of τ_{on} and τ_{off} of at least 4 s. In the case of *let-7a* and *let-7c* discrimination, an intensity threshold of 500 counts was used instead, and criterion (ii) was not applied as it would have eliminated a large fraction of *let-7c* molecules from analysis.

Kinetic Monte Carlo simulations of probe binding. SiMREPS probing of an immobilized target was simulated in MATLAB with the assumption of (pseudo-) first-order kinetics for both binding and dissociation. A random-number generator was used to make stochastic decisions as to whether a molecule will undergo a transition within discrete time steps of 0.5 s. The matrix of per-frame transition probabilities was generated from specified first-order rate constants. The number of transitions was recorded for each molecule for subsequent analysis (**Supplementary Note 2** and **Supplementary Fig. 10**).

PAGE assay of miRNA degradation in human serum. Synthetic miR-16 (final concentration 1 µM) was combined with sodium dodecyl sulfate (SDS, final concentration 0 or 2% w/v), proteinase K (New England BioLabs, final concentration 0, 0.08, 0.16, or 0.32 units/µl), and deionized water, then mixed with either PBS, pH 7.4 (final concentration 1×, Gibco) or human serum (final 50% v/v BioreclamationIVT) to a total volume of 20 µl. After 15 min incubation, samples were either left at room temperature or spiked with 2 µl EDTA (final concentration 20 mM) and heated to 90 °C for 2 min in a copper bath, then brought back to room temperature. Samples were incubated for 1 h more at room temperature, then separated on a denaturing, 8 M urea, 20% (w/v) polyacrylamide gel. The gel was stained using SYBR gold (Life Technologies) and imaged on a Typhoon 9410 Variable Mode Imager (GE Healthcare Life Sciences).

19. Michelotti, N., de Silva, C., Johnson-Buck, A.E., Manzo, A.J. & Walter, N.G. *Methods Enzymol.* **475**, 121–148 (2010).
20. Abelson, J. *et al. Nat. Struct. Mol. Biol.* **17**, 504–512 (2010).
21. Aitken, C.E., Marshall, R.A. & Puglisi, J.D. *Biophys. J.* **94**, 1826–1835 (2008).
22. Nicolai, C. & Sachs, F. *Biophys. Rev. Lett.* **8**, 191–211 (2013).

© 2015 Nature America, Inc. All rights reserved.